J|A|C|S
ARTICLES
Published on Web 05/27/2005

Understanding the Template Preorganization Step of an Artificial Arginine Receptor§

Barbara Kirchner* and Markus Reiher†

Contribution from the Theoretische Chemie, Institut für Physikalische und Theoretische Chemie, Universität Bonn, Wegelerstrasse 12, D-53115 Bonn, Germany

Received January 30, 2005; E-mail: kirchner@thch.uni-bonn.de

Abstract: A biomimetic complex which mimics the arginine−phosphonate diester interaction of the arginine fork is investigated with respect to structure and energetics of stable configurations. Within this work, we provide knowledge on local minima of the isolated system obtained from first-principles calculations. Non-negligible solvation effects are studied in a microsolvation approach. The interactions which govern the structural patterns of molecular recognition in this tweezer−guest complex can be significantly modulated by the action of hydrogen bond accepting and donating solvent molecules, such as dimethyl sulfoxide or water, which were present in experimental investigations on this system. Different tweezer−guest structures are evaluated with respect to their temperature-dependent thermodynamical properties as products of the first association reaction step of the bisphosphonate tweezer template and the guanidinium moiety.

1. Introduction

RNA−protein recognition plays an important role in various regulatory biochemical processes, but little is known about the detailed interactions at the molecular contact sites. A single arginine residue, the arginine fork, was identified to be required for specific binding[1] (see also refs 2 and 3). The interactions of arginine-rich proteins with phosphate and bases of RNA have been intensively investigated, and NMR spectroscopy is used for the structural characterization of the complexes in solution.[4−9] The potential pharmacological value of small receptor molecules, which recognize arginine-based guests, stimulated work on biomimetic systems.[10−14] Artificial receptors need to be designed such that the recognition of arginine residues is optimal. This requires a detailed understanding of the various interaction patterns between host and guest.

To tackle the challenging questions of the detailed modes of recognition in such systems, quantum chemical calculations can provide structural and (individual) energetical information not accessible to experimental techniques. However, one has to restrict such a study to a particular system, which resembles essential features of the whole class of tweezer−fork systems. The conclusions may then be generalized afterward. In this work, our focus will be on an artificial arginine receptor molecule developed by Schrader and co-workers.[12,15] This receptor complex **1** in Figure 1 consists of a bisphosphonate tweezer that clamps a guanidinium group of the guest (see also refs 16−18 for comparable bisphosphonate receptor molecules by Schrader et al.); the nomenclature is chosen as in ref 19. Structural and energetical information on this system has been obtained mainly from NMR investigations and, in part, from molecular mechanics calculations;[15] highly accurate calculations in a first-principles sense have not been carried out. The complex is designed to imitate the arginine−phosphonate diester interaction of the arginine fork,[1] which is a key element in RNA−protein recognition. The relevance of understanding the interaction modes of these arginine/guanidinium moieties with phosph[on]ate or sulf[on]ate residues has been very recently highlighted in the review by Schug and Lindner.[20]

A theoretical study by Frankel et al.[1] showed for the hydrogen network of the arginine fork a "side-on" arrangement (compare Figure 4 below), which was also proposed for the arginine bisphosphonate tweezer interaction within the artificial receptor system on the basis of molecular modeling studies.[12] However,

§ Part I of a series of papers on the "Development of a Thermochemical Model of Template-Assisted Chemical Processes".

† Present address: Institut für Physikalische Chemie, Helmholtzweg 4, D-07743 Jena, Germany.

(1) Calnan, B. J.; Tidor, B.; Biancalana, S.; Hudson, D.; Frankel, A. D. *Science* **1991**, *252*, 1167−1171.
(2) Ellington, A. D. *Curr. Biol.* **1993**, *3*, 375−377.
(3) Varani, G. *Acc. Chem. Res.* **1997**, *30*, 189−195.
(4) Battiste, J. L.; Mao, H.; Rao, N. S.; Tan, R.; Muhandiram, D. R.; Kay, L. E.; Frankel, A. D.; Williamson, J. R. *Science* **1996**, *273*, 1547−1551.
(5) Ye, X.; Gorin, A.; Ellington, A. D.; Patel, D. J. *Nat. Struct. Biol.* **1996**, *3*, 1026−1033.
(6) Brodsky, A. S.; Williamson, J. R. *J. Mol. Biol.* **1997**, *267*, 624−639.
(7) Legault, P.; Li, J.; Mogridge, J.; Kay, L. E.; Greenblatt, J. *Cell* **1998**, *93*, 289−299.
(8) Cai, Z.; Gorin, A.; Frederick, R.; Ye, X.; Hu, W.; Majumdar, A.; Kettani, A.; Patel, D. J. *Nat. Struct. Biol.* **1998**, *5*, 203−212.
(9) Patel, D. J. *Curr. Opin. Struct. Biol.* **1999**, *9*, 74−87.
(10) Lehn, J.-M.; Vierling, P.; Hayward, R. C. *J. Chem. Soc., Chem. Commun.* **1979**, 296−298.
(11) Eliseev, A. V.; Nelen, M. I. *J. Am. Chem. Soc.* **1997**, *119*, 1147−1148.
(12) Schrader, T. *Chem.−Eur. J.* **1997**, *3*, 1537−1541.
(13) Bell, T. W.; Khasanov, A. B.; Drew, M. G. B.; Filikov, A.; James, T. L. *Angew. Chem.* **1999**, *111*, 2705−2709.
(14) Ngola, S. M.; Kearney, P. C.; Mecozzi, S.; Russell, K.; Dougherty, D. A. *J. Am. Chem. Soc.* **1999**, *121*, 1192−1201.
(15) Rensing, S.; Arendt, M.; Springer, A.; Grawe, T.; Schrader, T. *J. Org. Chem.* **2001**, *66*, 5814−5821.
(16) Schrader, T. *J. Org. Chem.* **1998**, *63*, 264−272.
(17) Herm, M.; Schrader, T. *Chem.−Eur. J.* **2000**, *6*, 47−53.
(18) Herm, M.; Molt, O.; Schrader, T. *Chem.−Eur. J.* **2002**, *8*, 1485−1499.
(19) Gschwind, R. M.; Armbrüster, M.; Zubrzycki, I. Z. *J. Am. Chem. Soc.* **2004**, *126*, 10228−10229.
(20) Schug, K. A.; Lindner, W. *Chem. Rev.* **2005**, *105*, 67−113.

10.1021/ja050614+ CCC: $30.25

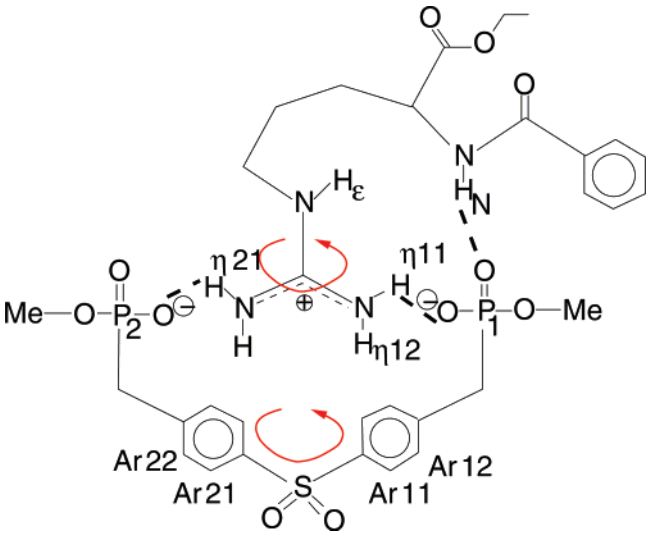

Figure 1. Lewis structure and notation of the biomimetic arginine receptor complex model **1**.

the approximations made in force field calculations question their reliability for the biomimetic complex under consideration where cooperative effects are important but neglected.

In contrast with the molecular mechanics findings, an NMR study on **1**[19] revealed a symmetrical end-on instead of a side-on interaction of the guanidinium moiety, which enables concerted rotations. Similar end-on interactions combined with concerted rotations were also found for arginine residues interacting with carboxylate groups in protein ligand complexes.[21] Molecular mechanics calculations in search for the global minimum structure confirmed the proposed side-on hydrogen bond network.[19] In this NMR study,[19] the complex under consideration served to develop an NMR method to measure scalar couplings across P═O···H−N hydrogen bonds, and the intermolecular hydrogen bonds in this artificial arginine receptor complex were directly determined via trans-hydrogen scalar couplings by NMR spectroscopy. A difficulty for the NMR experiments is that one has to freeze the substantial rotational motions of the complex, which is a general problem for supermolecular systems and often prevents their structural characterization. Since an X-ray structure of the complex is neither available nor desirable (as it does not necessarily equal the structure in solution), quantum chemical calculations are an inevitable source for structural information.

The aim of this study is twofold. On one hand, we want to shed light on the generic stability of different tweezer−fork configurations and their modulation by solvent molecules taken into account in a microsolvation approach. We treat these complexes with quantum chemical methods in order to resolve the discrepancies between experiment and molecular mechanics investigations especially regarding the side-on versus end-on debate. As this study is based on *first-principles* quantum chemical calculations, we avoid all uncertainties stemming from the classical force fields, which have been employed to obtain minimum structures in the above-mentioned molecular mechanics study.

On the other hand, the host−guest complex under consideration is an example for a template system, and the results obtained are relevant from the point of view of template chemistry. Template-assisted reactions are reactions in which a template induces a spatial preorganization of reactants prepared for a well-defined chemical reaction or molecular motion.[22−29] In view of the complexity of template-assisted chemical processes, quantum chemical approaches to molecular recognition have naturally been pursued only for specific systems (see, for example, ref 30[30] for a study of a molecular tweezer). The large number of local minimum configurations of host (template) and guest discussed in this work allows us to calculate thermodynamic functions needed as elements for a thermochemical model of template effects.[31] An essential step for this modeling is the investigation of the association reaction, for which the ratio of entropy difference times temperature, $T\Delta S$, with respect to enthalpy difference, ΔH, as well as the temperature dependence of entropy and enthalpy plays a decisive role.

The paper is organized as follows. The next section describes the quantum chemical methodology applied. After this, we discuss energies and structural patterns of different conformers. A detailed analysis of the hydrogen bond interaction patterns follows. The work concludes with a discussion of the structure characteristic molecular vibrations of the various complex configurations and of the temperature dependence of thermodynamic functions, which describe the thermochemical properties of the products of the template−substrate association reaction.

2. Quantum Chemical Methodology

For all quantum chemical structure optimizations, we used the density functional theory (DFT) programs provided by the TURBOMOLE 5.1 suite.[32] We chose the gradient-corrected density functional BP86[33,34] in combination with the RI density fitting technique.[35,36] The DFT results were obtained from all-electron restricted Kohn−Sham calculations. Ahlrichs' TZVP basis set has been used throughout, featuring a valence triple-ζ basis set with polarization functions on all atoms.[37] All interaction energies, which were calculated in a supermolecular ansatz, have been counterpoise corrected[38,39] in order to avoid basis set superposition effects. However, the counterpoise correction has not been included during structure optimization. The basis set superposition error turned out to be between 10 and 17 kJ/mol with Ahlrichs' TZVP basis set. The interactions in the tweezer−fork complex under consideration

(21) Nieto, P. M.; Birdsall, B.; Morgan, W. D.; Frenkiel, T. A.; Gargaro, A. R.; Feeney, J. J. *FEBS Lett.* **1997**, *405*, 16−20.

(22) Busch, D. H.; Stephenson, N. A. *Coord. Chem. Rev.* **1990**, *100*, 119.
(23) Anderson, S.; Anderson, H. L.; Sanders, J. K. M. *Acc. Chem. Res.* **1993**, *26*, 469.
(24) Cacciapaglia, R.; Mandolini, L. *Chem. Soc. Rev.* **1993**, *22*, 221.
(25) Hoss, R.; Vögtle, F. *Angew. Chem., Int. Ed. Engl.* **1994**, *33*, 375.
(26) Hubin, T. J.; Busch, D. H. *Coord. Chem. Rev.* **2000**, *200−202*, 5.
(27) Gerbeleu, N. V.; Arion, V. B.; Stang, P. J. *Template Synthesis of Macrocyclic Compounds*; Wiley-VCH: Weinheim, Germany, 1999.
(28) Diederich, F.; Stang, P. J. *Templated Organic Synthesis*; Wiley-VCH: Weinheim, Germany, 2000.
(29) Schalley, C. A.; Vögtle, F.; Dötz, K. H. *Templates in Chemistry I: Topics in Current Chemistry*; Springer-Verlag: Berlin, 2004.
(30) Ochsenfeld, C.; Koziol, F.; Brown, S. P.; Schaller, T.; Seelbach, U. P.; Klärner, F. *Solid State Nucl. Magn.* **2002**, *22*, 128−153.
(31) Kirchner, B.; Reiher, M. **2005**, to be submitted.
(32) Ahlrichs, R.; Bär, M.; Häser, M.; Horn, H.; Kölmel, C. *Chem. Phys. Lett.* **1989**, *162*, 165−169.
(33) Becke, A. D. *Phys. Rev. A* **1988**, *38*, 3098−3100.
(34) Perdew, J. P. *Phys. Rev. B* **1986**, *33*, 8822−8824.
(35) Eichkorn, K.; Treutler, O.; Öhm, H.; Häser, M.; Ahlrichs, R. *Chem. Phys. Lett.* **1995**, *240*, 283−290.
(36) Eichkorn, K.; Weigend, F.; Treutler, O.; Ahlrichs, R. *Theor. Chem. Acc.* **1997**, *97*, 119−124.
(37) Schäfer, A.; Huber, C.; Ahlrichs, R. *J. Chem. Phys.* **1994**, *100*, 5829−5835.
(38) Boys, S. F.; Bernardi, F. *Mol. Phys.* **1970**, *19*, 553−566.
(39) van Duijneveldt, F. B.; van Duijenveldt-van de Rijdt, J. G. C. M.; van Lenthe, J. H. *Chem. Rev.* **1994**, *94*, 1873.

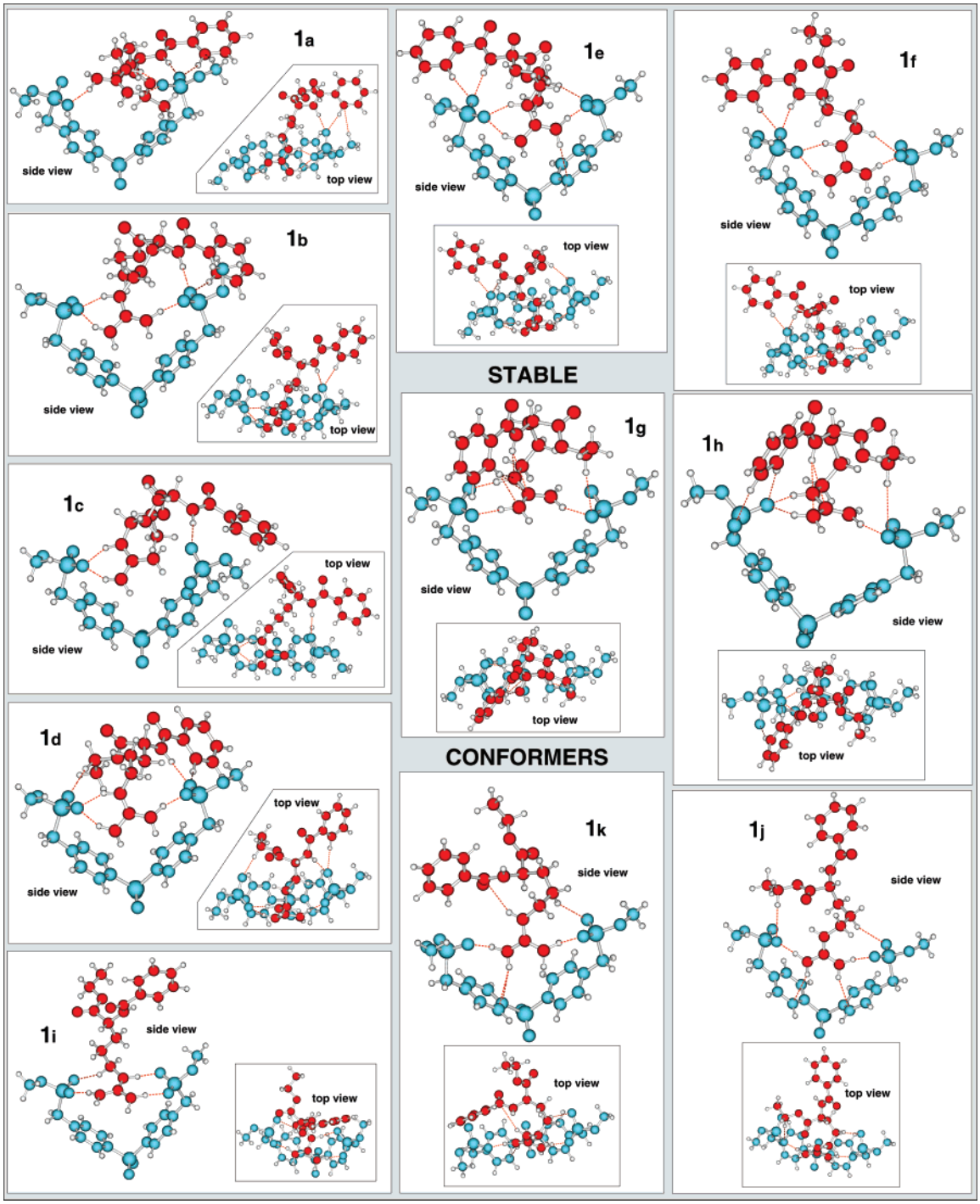

Figure 2. Conformers of the isolated artificial arginine fork system **1** as obtained from structure optimizations (guanidinium moieties are colored red and bisphosphonate tweezers blue). Dotted red lines do not necessarily correspond to hydrogen bonds, but denote short contacts and thus mark close geometrical arrangements.

are modulated by surrounding polar solvent molecules. To probe this effect, we use a microsolvation approach, in which single solvent molecules are placed close to important hydrogen donor and acceptor sites. In view of our previous cluster studies, important details of the solvent effects are described sufficiently well already at the microsolvation level.[40,41] The vibrational frequencies and the zero-point vibrational energies ΔZPE are obtained within the harmonic approximation. The second derivatives of the total electronic energy were computed as numerical first derivatives of analytic energy gradients with the program SNF.[42] The harmonic frequencies are also used to calculate the vibrational contribution to the entropy, while the rotational contribution is calculated in the standard way from the moments of inertia of the rigid rotor. For additional comments on the quantum chemical procedures, see the Supporting Information.

3. Conformer Structures and Interaction Energies

We first investigated several isomeric structures of the *isolated* artificial arginine receptor complex **1** in order to

(40) Kirchner, B.; Reiher, M. *J. Am. Chem. Soc.* **2002**, *124*, 6206−6215.
(41) Odelius, M.; Kirchner, B.; Hutter, J. *J. Phys. Chem. A* **2004**, *108*, 2044−2052.
(42) Neugebauer, J.; Reiher, M.; Kind, C.; Hess, B. A. *J. Comput. Chem.* **2002**, *23*, 895−910.

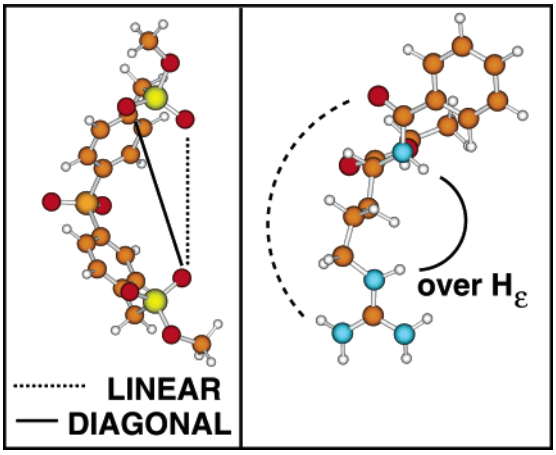

Figure 3. Left: Schematic drawing of the bisphosphonate receptor with a diagonal or a linear hydrogen bonding pattern. Right: Guanidinium fork bending the amide proton of the N−H group over H_ϵ. See text for further explanation.

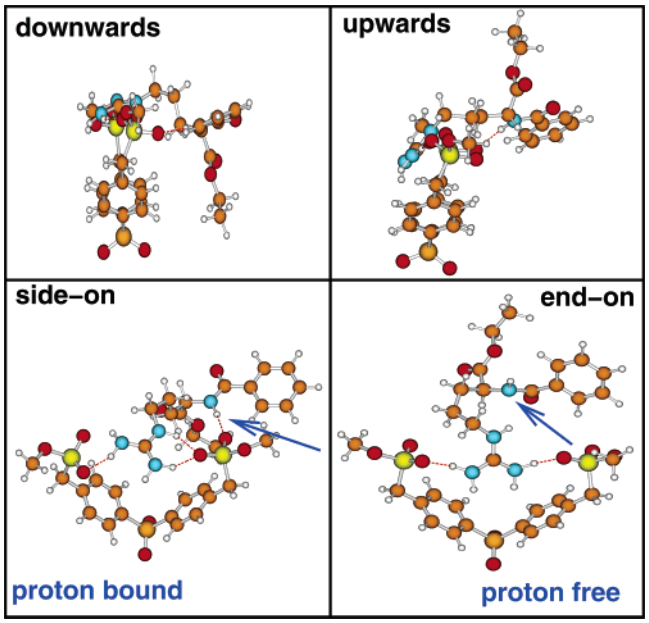

Figure 4. Structural characteristics of complex **1**. Upper left panel: Ester group points downward. Upper right panel: Ester group points upward (pattern 3). Lower panel (patterns 4 and 5): Side-on and H_N bound (left); end-on and proton H_N unbound (right).

determine the intrinsically most stable structure at zero temperature and to understand the basic structural patterns. The conformers in Figure 2 were obtained by carrying out geometry optimizations starting from different structures, which resemble experimental findings.

3.1. Structure Characteristic Bonding Patterns. The most important types of structural patterns, which can be observed in the optimized conformer structures of **1**, are listed in the following questions. Some of these questions could not be answered by experiment.

Option 1: Is the diagonal arrangement for the connection of phosphonate−arginine−phosphonate energetically preferable over the linear one? Figure 3 (left scheme) demonstrates how the two sides of the arginine fork can be bound linearly or diagonally. From the experimental point of view, neither of these arrangements has been ruled out yet.

Option 2: Is the amide proton H_N bound to the phosphonate receptor? Figure 4 indicates this situation in the lower panels by blue arrows. Via NMR spectroscopy, a hydrogen bond between the amide proton of arginine and one of the phosphonate moieties was directly detected.[19]

Option 3: Especially relevant is the question whether the arginine fork is bent over the H_ϵ if the amide proton H_N forms a hydrogen bond to the bisphosphonate unit. In Figure 3 (right-hand side), the line indicates how the amide group of the protected amino acid could be connected to one bisphosphonate unit. The experimental findings indicate the preference of the N−H group to form a hydrogen bond over the H_ϵ atom.[19]

Option 4: Does the ester group of the arginine fork point downward or upward (see Figure 4 upper left and right panels)?

Option 5: Is the side-on instead of the end-on structure preferred? In other words, is the H_ϵ hydrogen bound to the phosphonate group (= side-on)? The lower panel of Figure 4 shows a side-on conformer (left) as opposed to an end-on conformer (right). The NMR experiment[19] confirms an end-on structure at finite temperature. As will be shown, this might be a structural pattern where solvent effects are decisive.

Option 6: Are the guanidinium protons H_ϵ and $H_{\eta^{11}}$ hydrogen bound to the same acceptor phosphonate oxygen atom, that is, is a 2-fold hydrogen bridge[43] built?

3.2. Definition of Interaction Energies. For the energetical classification of the optimized structures, we used the following (standard) interaction energy definitions. Interactions energies (IEs) have been calculated within the supermolecular approach

$$\mathrm{IE}_i = E_{\mathrm{complex}_i} - [E_{\mathrm{fork}_i} + E_{\mathrm{tweezer}_i}]_{\mathrm{frozen}} \qquad (1)$$

in order to determine the total strength of the various bonding patterns between the guanidinium group and the bisphosphonate receptor part of a complex conformer *i* at (frozen) structures as adopted in the complex. Comparing the IEs, which are calculated at these *unrelaxed* monomer structures, yields the intrinsic interaction strength. These energies neglect intramolecular relaxation effects of template and guest, which would reduce the interaction energy. In addition to the supermolecular approach, we employ the SEN method[44,45] to detect and quantify the interaction energies of individual hydrogen bonds

$$\mathrm{IE}^{\mathrm{SEN}}_{\mathrm{HA},i} = \lambda \sigma_{\mathrm{HA},i} \qquad (2)$$

in nondecomposable systems, which are not accessible by the supermolecular approach; λ was adjusted to a test set of hydrogen-bonded complexes.[44] For comparison, we calculated differences in interaction energies with respect to a reference structure:

$$\Delta\mathrm{IE}_i = \mathrm{IE}_i - \mathrm{IE}_{\mathrm{ref}} \qquad (3)$$

As reference, we chose the conformer with the largest total energy in absolute value. Energies, which also incorporate the structural relaxation of the fragments, can be defined as

(43) Reckien, W.; Peyerimhoff, S. D. *J. Phys. Chem. A* **2003**, *107*, 9634−9640.
(44) Reiher, M.; Sellmann, D.; Hess, B. A. *Theor. Chem. Acc.* **2001**, *106*, 379−392.
(45) Reiher, M.; Kirchner, B. *J. Phys. Chem. A* **2003**, *107*, 4141−4146.

Table 1. Differences in Total Energy ($\Delta D_{e,i}$), Zero-Point Vibrational Energy Corrected Total Energy Difference ($\Delta D_{0,i}$) (reference complexes **1a** and **2a**, respectively) and Relative Interaction Energies (ΔIE_i) as Calculated within the Supermolecular Approach (see section 3.2.)[a]

complex	$\Delta D_{e,i}$	$\Delta D_{0,i}$	ΔIE_i
	Isolated Tweezer−Fork Complexes		
1a	0	0	0
1b	8.9	19.6	−0.8
1c	10.9	7.5	−1.1
1d	12.2	13.5	7.9
1e	16.1	12.2	0.3
1f	18.4	13.5	7.2
1g	24.6	37.7	−14.7
1h	39.2	34.5	8.3
1i	39.3	36.8	43.7
1j	55.2	48.1	101.1
1k	88.9	126.8	121.6
	+1 DMSO Molecule (microsolvation)		
2a	0	0	0
2b	11.2	11.0	3.6
2c	13.7	13.0	4.6
2d	51.2	47.2	64.8

[a] All energies are given at 0 K and in kJ/mol (see the Supporting Information for additional data).

differences between total electronic energies of minimum structures

$$D_{e,i} = E_{\text{complex}_i} - [E_{\text{fork}} + E_{\text{tweezer}}]_{\text{relaxed}} \quad (4)$$

or as relative total energies

$$\Delta D_{e,i} = D_{e,i} - D_{e,\text{ref}} = E_{\text{complex}_i} - E_{\text{ref}} \quad (5)$$

For the calculation of the D_0 values, the zero-point energy differences have been added to the total electronic energy differences

$$D_0 = D_e + \text{ZPE} \quad (6)$$

which allow the calculation of zero-temperature-corrected relative energies,

$$\Delta D_{0,i} = \Delta D_{e,i} + \Delta \text{ZPE}_i \quad (7)$$

for the comparison of different optimized conformer structures.

3.3. Relative Conformer Energies. Table 1 lists different types of interaction energies at 0 K for all conformers as obtained from supermolecular calculations. The optimized structure **1a** agrees with experiment in two out of three structure patterns, and most importantly, it coincides with the previously found theoretical minimum structure (side-on).[19] In our calculations on the isolated system, this conformation is also energetically most favorable. Therefore, we choose it as a reference to compare with all other conformers. In **1a**, the guanidinium unit is linearly connected between the two phosphonate groups, and the fork is bent via the H_ϵ hydrogen atom; the ester group points downward, and it is a side-on structure. The amide proton (H_N) takes part in hydrogen bonding at the phosphonate group, and the H_ϵ and H_η[11] protons form a 2-fold hydrogen bond; see also the first picture on the left of Figure 2. The two individual parts of this conformer (guanidinium moiety and phosphonate tweezer, respectively) are bound rather strongly by −817.8 kJ/mol, which exceeds a normal hydrogen bond interaction energy by far. This is due to strong electrostatic monopole−monopole interactions of the charged parts (formally, we have two negative charges for the phosphonate tweezer and one positive charge on the guanidinium group).

Although **1b**−**1d** are equal in all six structure characteristic elements listed above, they differ in other atomic arrangements, which makes them different local minima on the potential energy surface. Comparing these conformers to **1a** gives an estimate for the energy amount needed to bend the protected amino acid rest the other way around, that is, not over H_ϵ. This amount of energy could be important for a possible rotation of the ester group around the guanidinium rest (as the rotation of the guanidinium rest might not be concerted with the H_ϵ proton, both moieties are supposed to rotate). It only leads to a mild increase in total energy by 12.2 kJ/mol for **1d**, 10.9 kJ/mol for **1c**, and only 8.9 kJ/mol for **1b** (see Table 1, first column). For conformer **1b** and **1c**, we even find a similar (intrinsic) interaction energy IE as for the reference conformer **1a**, although the total energy comparison shows that structural relaxation makes them relative to **1a** less favorable. We will later discuss the detailed differences between **1b** and **1d** when we consider geometries and hydrogen bonds. To move the ester group of the guanidinium group upward (i.e., comparing **1f** with **1a**) costs 18.4 kJ/mol in total energy and results in a loss of 7.2 kJ/mol (intrinsic) interaction energy IE. Note that **1e** is similar to **1a**, and both can be considered closely (though not completely) related through a mirror operation.

Breaking the hydrogen bond of H_N from the guanidinium unit can be considered by comparing structures **1i** and **1f**. All patterns are the same except for the second and sixth. Breaking this bond leads to a loss of 20.9 kJ/mol in total energy and of 36.5 kJ/mol in interaction energy IE. This is in accordance with results of Schrader et al.,[15] where stronger association constants and free binding enthalpies were found for the guanidinium rest under consideration as compared to that of a guanidinium group with methyl rest, where no H_N group is present. Unbound H_N protons are also found in two other important complex structures. These are the two conformers that are not side-on but end-on structures. Conformers **1j** and **1k** lie 55.2 and 88.9 kJ/mol above the side-on structure **1a**. Taking the unbound H_N into account, we can estimate the difference between side-on and end-on structures by comparing the end-on structure **1k** to the side-on conformer **1i**. Conformer **1i** agrees in all structural patterns with the end-on structures, except that it is a side-on structure. The increase from side-on to end-on in total energy is then found to be 49.6 kJ/mol (D_e(**1*k***) − D_e(**1*i***)). The interaction energy increases by 77.9 kJ/mol (IE(**1*k***) − IE(**1*i***)).

Another interesting structure feature is exhibited in complexes **1h** and **1g**. Here, the H_N hydrogen atom binds to a nitrogen atom of the guanidinium group. Conformer **1h** is also the only example for a diagonal structure. In view of the structural patterns, **1a** and **1e** seem to possess very similar structures, although they are, with respect to ΔD_e, different. The section on hydrogen bond interactions will explain this seemingly discrepancy.

3.4. Microsolvation Effects. In experiment, the complex is solvated in a mixture of 10% deuterated dimethyl sulfoxide (DMSO) in deuterated CH_2Cl_2, which is the reason we also added one DMSO molecule in order to model microsolvation. Figure 5 depicts microsolvated conformers (1 DMSO **2** and,

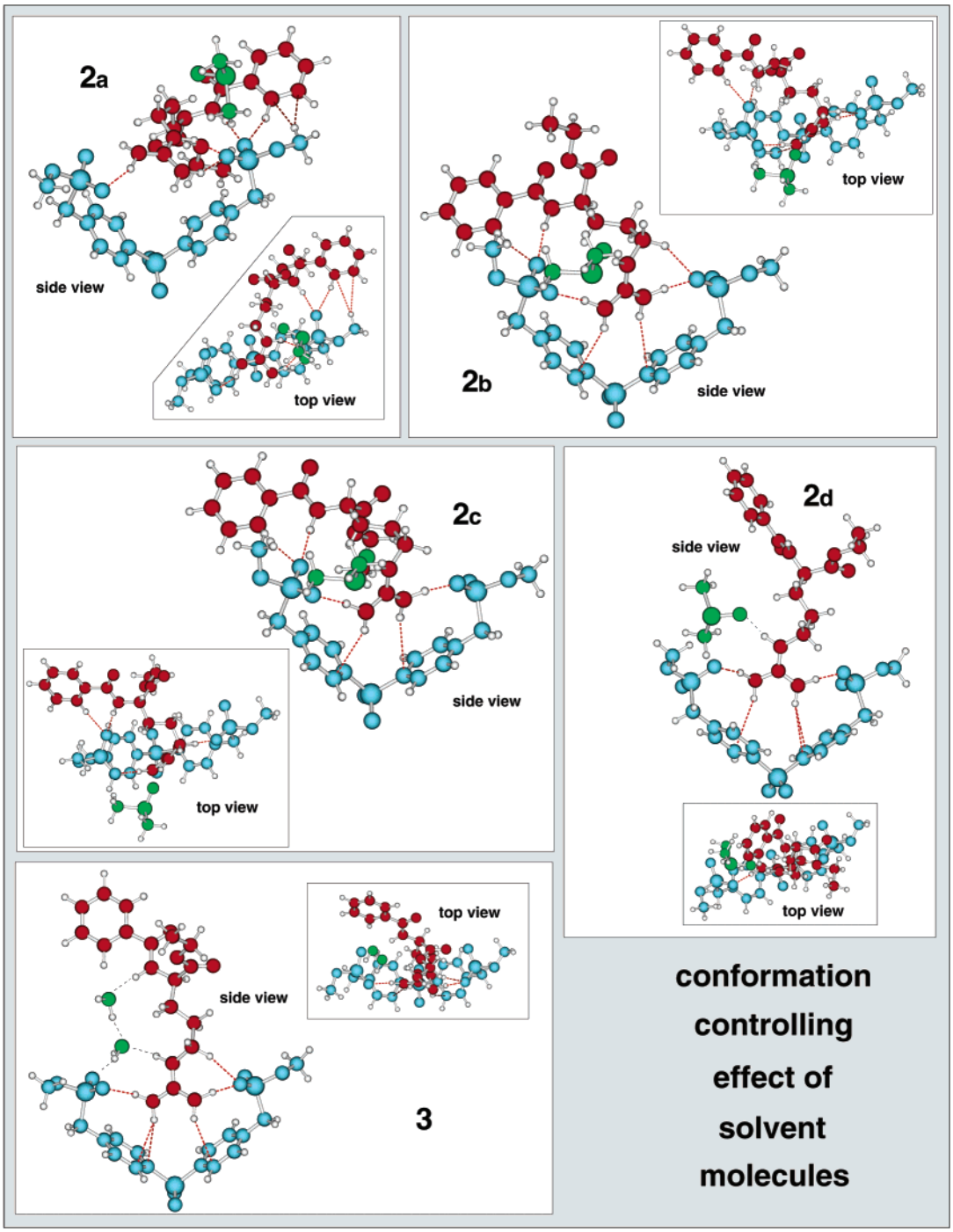

Figure 5. Conformers of the microsolvated artificial arginine fork system **2a**−**d** (+1 DMSO) and **3** (+2H_2O) as obtained from structure optimizations.

for comparison, 2H_2O **3** added); interaction energies for these complexes are given in Table 1. We consider DMSO associated to the guanidinium part in the calculation of the interaction energies. Hence, we consider the complex built up by two units instead of three units. A natural docking position for the DMSO oxygen atom would be the H_ϵ proton in order to enforce an end-on structure. As a result, the interaction energy between the guanidinium and the bisphosphonate will be weakened.

To compare the DMSO conformers, we choose, again, the one with the lowest total energy as reference point. This structure **2a** is similar to that of the side-on unsolvated complex **1a**. Within the DMSO complexes, the interaction energy is weakened by up to 64.8 kJ/mol. Compare **2a** to **2d**, which forms a hydrogen bond between H_ϵ and the oxygen atom of DMSO. The structure changes thus from side-on to end-on, and the interaction energy becomes much smaller. As already mentioned, there is a hydrogen bond at H_ϵ, which will later be discussed in section 4. Furthermore, it is interesting that the difference in total interaction energy between the DMSO solvated side-on **2a** and the DMSO solvated end-on structure **2b** is only 11 kJ/mol and the difference in interaction energy is even less, namely, 3.6 kJ/mol (compare **2a** and **2b** in Table 1).

To summarize, changing any of the structural pattern listed above costs less than 10−40 kJ/mol in total energy. The energy

Table 2. Hydrogen Bond Energies IE_i^{SEN} as Calculated with the Shared-Electron Number Approach of refs 44 and 45 in kJ/mol (distances in picometers and angles in degrees)

complex	IE_i^{SEN} (H_ϵ)	IE_i^{SEN} (H_N)	IE_i^{SEN} (H_{η}^{11})	IE_i^{SEN} (H_{η}^{21})	IE_i^{SEN} (H_{η}^{22})
Isolated Tweezer−Fork Complexes					
1a	28.5	15.4	16.3	17.4	25.3
1b	21.6	17.1	29.0	46.8	
1c	28.0	10.9	22.8	13.1	20.9
1d	19.2	15.1	30.7	45.1	
1e	18.9	11.9	23.8	57.6	
1f	17.0	15.9	23.8	60.2	
1g	44.2	9.6	34.7	11.6	28.5
1h	28.7	7.4	20.7	10.4	35.2
1i	32.9		38.1	45.6	
1j			43.2	50.8	
1k			49.6	54.8	
+1 DMSO					
2a	23.0	13.9	15.8	15.4	26.2
2b	18.6	16.3	33.4	53.1	
2c	19.7	14.4	34.7	54.0	
2d	18.3		39.1	52.0	
+2 H_2O					
3	13.5	16.0	26.6	68.6	

difference between the experimentally expected end-on structure and a side-on structure is significantly reduced from about 50 kJ/mol (for the isolated species) to approximately 10 kJ/mol if microsolvation is taken into account.

4. Patterns of Cooperative Hydrogen Bonds

From the linear relation between the shared electron number and the interaction energy (SEN approach), we now derive strengths for local (individual) hydrogen bonds in the arginine receptor complex. The results are collected in Table 2, which gives the hydrogen bonding of the H_ϵ, H_N, H_{η}^{11}, H_{η}^{22}, and H_{η}^{21} protons (for additional details on hydrogen bond lengths and angles, see the Supporting Information).

We do not observe hydrogen bonding to H_ϵ and H_N in either end-on conformers **1j** and **1k** as opposed to experiment. The situation changes in the case where we fed the H_ϵ with the solvent molecule. Here, we obtain a hydrogen bond to this proton of 18.3 kJ/mol (**2d**) and 18.6 kJ/mol (**2b**) SEN interaction energy, which is in the range of a water−water hydrogen bond. The strongest H_ϵ bond is found in **1g** (side-on) with 44.2 kJ/mol. This conformer provides a remarkable hydrogen bond acceptor for H_N, namely, the nitrogen atom binding H_ϵ of the guanidinium moiety. The hydrogen bonds to H_N are always weaker than those to H_ϵ (an exception is structure **3**, which is due to a more favorable arrangement that is possible because two solvent molecules come into play); the H_N bonds range from 7 to 17 kJ/mol, which could be relevant for the rotation of the ester group since a weak hydrogen bond is more easily broken. In contrast to the experimental findings, the strongest bond to H_N is obtained for the structure where the guanidinium rest is not bent over the H_ϵ in **1b**. In the last section, we have compared the interaction energies of **1i** and **1f** and deduced that breaking of the H_N hydrogen bond results in an energy increase of 36.5 kJ/mol. The SEN analysis gives significantly smaller values for these hydrogen bonds (7−17 kJ/mol; see Table 2). This might imply that additional weak interactions must be broken when rearranging, for example, the conformer **1i** to **1f** such that no hydrogen bond of the hydrogen atom H_N to the phosphonate group can be formed.

The H_{η}^{11} protons are bound by up to 16−50 kJ/mol. They are usually stronger than H_N or H_ϵ bonds. The strongest hydrogen bonds occur in the end-on conformers **1j** and **1h**. For these complexes, it is possible to arrange the protons in a geometrically more favorable way than in the side-on structures; see for instance, complex **1k**, where the hydrogen bond length is 160 pm and the donor−proton−acceptor angle is 170.4°. The side-on structures never exhibit such short hydrogen bonds, and none of them arranges as linear as **1j** with 177.9°. H_{η}^{21} shows the broadest energetical variety; hydrogen bonds from 10 to 60 kJ/mol are possible. The weaker bonds of H_{η}^{21} are those where the H_{η}^{22} proton is also forming hydrogen bonds. The stronger bonds of H_{η}^{21} are the ones in those configurations which are end-on structures and also in side-on complexes where H_{η}^{22} is not forming hydrogen bonds. This explains the difference between the seemingly similar structures **1a** and **1e**; **1a** forms a hydrogen bond with H_{η}^{22}, while **1e** does not.

So far, the isolated molecule calculations led to several contradictions when compared to experiment. The situation changes when we consider complexes which have been microsolvated with one DMSO molecule. For the DMSO complexes **2d** and **2b**, where the solvent molecule forms the hydrogen bond to H_ϵ, we obtain an interaction energy of approximately 18 kJ/mol. Thus, the solvent molecule can easily compete with the phosphonate group regarding a bond to H_ϵ (and H_N) so that the end-on structure element becomes more likely when solvent molecules are involved. All hydrogen bond strengths are in the range of those for water−water hydrogen bond energies, and one can imagine that at ambient temperature, these bonds can be easily broken to perform the experimentally proposed rotation. Whereas in the isolated system the end-on structures, which are very important from the experimental point of view, exhibited neither H_ϵ nor H_N hydrogen bonds, the microsolvated system does indeed show such a hydrogen bond pattern.

5. Vibrational Signatures of Different Conformers

Turning now to vibrational analyses of all optimized structures, we find characteristic bands in the calculated IR spectra, which might allow an in situ structure determination of the complex in experiment that can be used to complement the findings in NMR spectroscopy. These predicted feature bands are highlighted for five selected structures in Figure 6.

The main difference between the structures, whose vibrational spectra are plotted in Figure 6, is structural pattern No. 4: **1a**, **1d**, and **1i** are side-on conformers, while **1j** and **1k** are end-on conformers. However, the similarity of the conformers gradually decreases. The green letters A, B, C, D, ... and corresponding boxes in Figure 6 denote structure characteristic vibrations (for wavenumbers and mode pictures, see the Supporting Information):

Type A: These vibrations occur at 438 cm^{-1} for **1a** and at 482 cm^{-1} for **1i**. The modes consist of a symmetric $N-H_{\eta}^{22}$ and $N-H_{\eta}^{12}$ out-of-plane movement relative to the phosphonate tweezer and are only present in side-on structures, which are oriented approximately parallel to the bisphosphonate plane. Opposed to this, the end-on conformers **1d** are oriented in an orthogonal plane and thus do not show vibrations of type A. The blue shift of **1i** relative to **1a** is likely to be due to the fact that H_{η}^{22} forms no strong hydrogen bond in **1i**.

Type B: Another feature which is absent in the end-on complexes occurs between 800 and 900 cm^{-1} and is, again,

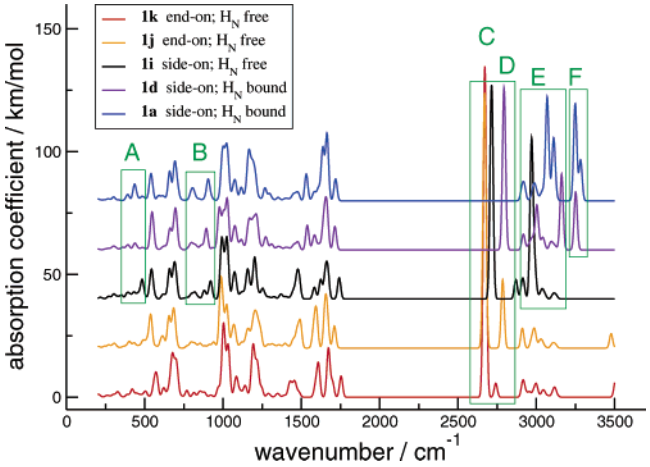

Figure 6. Calculated infrared spectra of five typical conformers **1a**, **1d**, **1i**, **1j**, and **1k** (intensities have been Gaussian broadened). Green letters and boxes mark structure characteristic vibrations which are discussed in the text.

due to an out-of-plane wagging motion of the guanidinium protons. The vibrations at shorter wavenumber involve both $H_{\eta^{11}}$ and H_{ϵ}, the ones at larger wavenumber $H_{\eta^{22}}$ and $H_{\eta^{21}}$.

Type C: Type C modes do not appear in the spectra of side-on complexes. It is a $N-H_{\eta^{11}}$ and $N-H_{\eta^{21}}$ asymmetric stretching mode.

Type D: This peak is also characteristic for the end-on structure element, though it shows only little IR intensity in the end-on conformer **1k**. The vibrations of type D are the symmetric counterparts of the C modes.

Type E: These vibrational features are only present in the side-on complexes and involve $N-H_{\epsilon}$ and $N-H_{\eta^{11}}$ stretching modes. The peak is blue-shifted for **1d** relative to **1a**; **1a** forms a stronger hydrogen bond with H_{ϵ} than does **1d**. A red shift occurs for **1i** relative to **1a**, where **1a** forms a weaker hydrogen bond at H_{ϵ} than does **1i** (compare also Table 2).

Type F: The last feature stems from the stretching vibration of the $N-H_N$ bond. In principle, it could also occur in end-on conformers if they can be arranged such that H_N forms a hydrogen bond with the bisphosphonate group.

6. Thermochemical Analysis

The temperature dependence of entropy S and enthalpy H yields first insight into the basic thermodynamical properties of the template−substrate system **1**. On the basis of the Gibbs−Helmholtz equation

$$\Delta G(T) = \Delta H(T) - T\Delta S(T) \qquad (8)$$

the thermodynamic quantities of a given conformer are related to those of a reference structure (i.e., to structure **1a** in this case). For the elementary association step A in a template-assisted reaction,[31] one would assume that the association entropy, ΔS_A, is negative as the entropy of the whole system is expected to decrease because of orienting and ordering effects of the template. For this initial step A to be exergonic, ΔG_A would have to be negative. This immediately implies that the enthalpy contribution, ΔH_A, which has its roots in the attractive intermolecular interactions of template and substrate, needs to be larger than the entropy loss, $T\Delta S_A$. However, this simple picture neglects several important issues. Most important is that no unique association reaction exists due to the floppy nature of the complex structure and the weak interactions that make template and substrate stick together. However, we may regard the optimized complex structures as the products of all imaginable association reactions. Then, the difference of the thermodynamic quantities of these product structures gives the relative thermodynamic stabilities of these products.

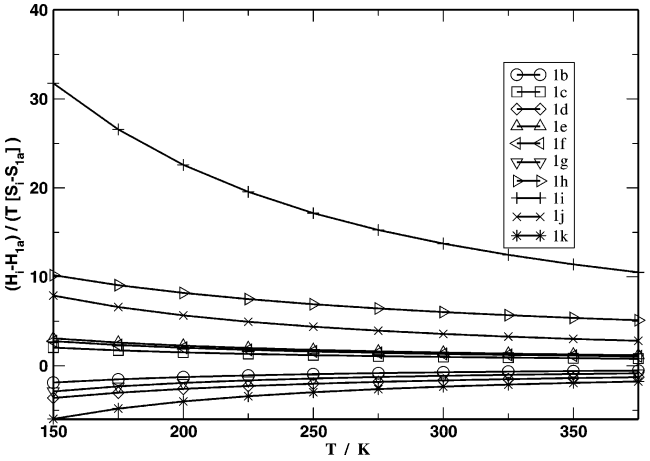

Figure 7. Dependence of ratio ΔH and $T\Delta S$ of the isolated conformers relative to structure **1a**.

To investigate whether the strong temperature dependence of the entropies of the different structures can be decisive for the stabilization of a certain conformation at a given temperature, one has to compare the magnitudes of $T\Delta S$ and ΔH. This comparison has been carried out, and the results are shown in Figure 7. In view of the approximations inherent in the thermodynamic functions and of the isolated nature of the configurations, we may deduce from the calculation of these ratios that the entropy effect can be of the order of the enthalpy difference so that rearrangements are likely for certain configurations.

7. Conclusions

We presented the first detailed quantum chemical study on the template−guest recognition patterns within the biomimetic arginine receptor complex **1**. The DFT methods employed are an appropriate means to study the different types of interactions, which are all dominated by electrostatic contributions. The main advantage of this approach is that it properly accounts for cooperative effects (i.e., many-body and polarization effects), which have been neglected in previous calculations with plain force field methods. Apart from the discussion of minimum structures of the bisphosphonate−guanidinium complex **1**, which clarified structural issues unresolved in previous work, we carried out vibrational analyses from which we extracted structure characteristic vibrational modes. The predicted wavenumbers of these modes may allow testing of the side-on or end-on interaction pattern in situ. Such experimental data can complement the NMR results.

The intrinsic interactions within complex **1** are now well understood. We were able to classify six important structure patterns, which characterize this system, and to determine the energetical differences between these structural patterns. For a complete understanding, a detailed hydrogen bond energy discussion was necessary, which we performed on the basis of the SEN approach. We initially found a side-on orientation to be most favorable in *isolated* complex structures. However,

taking only the hydrogen bonds into account reveals that an end-on arrangement would have been preferred. This might be the reason aprotic polar solvents turned out to favor the end-on pattern. Furthermore, a decrease of the energetical difference between the intermolecular attraction patterns was induced by solvent molecules in the microsolvation studies. Complex **1** is thus a nice example, where solvent molecules play a significant role in the modulation of the hydrogen bond patterns in **1**; compare also the review by Cooke and Rotello,[46] which highlights such effects on structure and function in biological systems. Choosing an aprotic but hydrogen-bond-accepting solvent should enhance the concentration of end-on structures.

The relative stability of the different structures is important for the possible association reactions of tweezer and guest leading to complex **1**. This relative stability is governed by temperature-dependent enthalpic and entropic contributions, which we investigated within our quantum chemical standard model. While enthalpy differences are small (and governed almost solely by the electronic energy difference), they can be compensated by entropy effects so that rearrangement reactions (particularly in solution) become very likely. This result supports the experimentally suggested rotation of the guanidinium residue within the complex.[19]

Although the results presented have been obtained for the particular biomimetic model **1**, they can be transferred to similar receptors for the binding of arginine-based guests because of the explicit analysis of the energy range of various hydrogen bond contacts. Moreover, the analysis demonstrates that no singular chemical structure can be indentified to represent such a complex in solution. Instead, several structural motifs need to be taken into account, and the reaction conditions may favor one over the other. This implies that experimental results are highly dependent on the solvent.

Acknowledgment. We dedicate this work to the memory of our academic teacher and friend Professor Bernd Artur Hess who passed away in summer 2004. We thank Prof. R. M. Gschwind for many helpful discussions. This work has been financially supported by the collaborative research center SFB 624 “Templates”, by the Fonds der Chemischen Industrie, and by the Forschungskredit Zürich.

Supporting Information Available: Quantum chemical methodology, additional information on conformer structures and interaction energies, data on cooperative hydrogen bonds, vibrational signatures of different conformers, thermochemical analysis, and Cartesian coordinates, total energies, and ZPEs. This material is available free of charge via the Internet at http://pubs.acs.org.

JA050614+

(46) Cooke, G.; Rotello, V. M. *Chem. Soc. Rev.* **2002**, *31*, 275−286.